



Nitrogen processing in the hyporheic zone of a pastoral stream

RICHARD G. STOREY, D. DUDLEY WILLIAMS*
and ROBERTA R. FULTHORPE

*Division of Life Sciences, University of Toronto at Scarborough, 1265 Military Trail, Scarborough, Ontario, M1C 1A4, Canada; *Author for correspondence (e-mail: williamsdd@utsc.utoronto.ca; phone/fax: 1-416-287-7423)*

Received 17 October 2002; accepted in revised form 21 August 2003

Key words: Denitrification, DNRA, Hyporheic zone, Nitrification, Nutrient dynamics, Stream ecology

Abstract. The distribution of nitrogen-transforming processes, and factors controlling their rates, were determined within the hyporheic zone of a lowland stream draining agricultural land. In the field, physicochemical parameters were measured along a 10 m-long hyporheic flow line between downwelling and upwelling zones. Sediment cores were retrieved from the stream bed surface, and from 20, 40 and 60 cm deep in each zone, and in the laboratory, water from the corresponding depth was percolated through each core at the natural flow rate. Concentrations of nitrogen species and oxygen were measured before and after flow through each core. Denitrification was measured using a ^{15}N -nitrate tracer. Shallow and downwelling zone samples were clearly distinct from deeper and upwelling zone samples in terms of physicochemical conditions, microbial processes and factors controlling nitrogen processing. Denitrification was highest in surface and downwelling zone cores, despite high oxygen levels, probably due to high pore-water nitrate concentrations in these cores and isolation of the denitrifying bacteria from oxygen in the bulk water by the hyporheic biofilms. Denitrification was limited by oxygen inhibition in the downwelling group, and by nitrate availability in the upwelling group. Strong evidence indicated that dissimilatory nitrate reduction to ammonium, occurred in almost all cores, and outcompeted denitrification for nitrate. In contrast, nitrification was undetectable in all but two cores, probably because of intense competition for oxygen. Field patterns and lab experiments indicated that the hyporheic zone at this moderately N-rich site is a strong sink for nitrate, fitting current theories that predict where hyporheic zones are nitrate sinks or nitrate sources.

Introduction

Recent work in hyporheic ecology and biogeochemistry has emphasised the importance of comparing hyporheic zone functioning in different stream types (Stanley and Jones 2000). One reason is to establish where, why and in what ways the hyporheic zone significantly influences whole system energetics and nutrient spiralling. Studies to date (e.g., Duff and Triska 1990; Triska et al. 1990; Jones et al. 1995; McMahon et al. 1995; Holmes et al. 1996; Wondzell and Swanson 1996; Hill et al. 1998; Chestnut and McDowell 2000; Hinkle et al. 2001) have shown that nitrogen dynamics operate quite differently in different stream systems. Nitrogen cycling processes and rates depend on subsurface physicochemical conditions, including the balance between downwelling surface water and upwelling ground-

water, the concentrations of nitrate, ammonium and organic carbon in advected water, and the hydraulic conductivity of the hyporheic sediments.

Despite the growing number of studies describing nutrient transformations along subsurface flow paths, some fundamental questions remain, such as what conditions determine whether the hyporheic zone will be a source or a sink of nitrogen (Dent et al. 2000). This question remains partly because most investigations to date have focused on streams where subsurface nitrification, either from ammonified organic nitrogen or from ammonium-rich groundwater, is the major source of nitrate. In contrast to these studies, where the hyporheic zone exported nitrate, Hill et al. (1998) found that in a N-rich agricultural stream, the hyporheic zone acted as a sink. This confirmed the prediction by Jones and Holmes (1996), that the hyporheic zone of N-poor streams would generally be a source of nitrate and the hyporheic zone of N-rich streams a sink. However, it also highlighted the importance of further studies in N-rich streams.

Initial studies in the Speed River, southern Ontario (Storey 2001), had shown that conditions in this stream were different, in at least one aspect, to those in each of the streams studied to date. At a headwater riffle-pool unit in the Speed River, surface water was moderately high in nitrate, whereas groundwater was relatively low in total nitrogen. In contrast, most previous studies have been conducted in low-nitrate streams (e.g., Triska et al. 1993; Wondzell and Swanson 1996), or where the main nitrogen source was groundwater ammonium (Shingobee River; Duff and Triska 2000), or groundwater or surface water DON (e.g., Jones et al. 1995). The hyporheic zone received downwelling surface water to at least 1 m deep at the upstream end of the riffle, but the permeability of stream bed sediments was low compared to other streams studied (e.g., Triska et al. 1993; Jones et al. 1995), producing low subsurface flow rates. The patterns of physicochemical changes along hyporheic flow lines also were different; nitrate, ammonium, DO and DOC concentrations decreased together to almost zero between downwelling and upwelling zones in the mid-channel, whereas in other studies (e.g., Jones et al. 1995; Wondzell and Swanson 1996; Hill et al. 1998) nitrate and/or ammonium have increased, and oxygen typically has remained moderately high. These differences raise the question of whether the distribution and rates of different nitrogen-transforming processes in this Speed River site match those in other studies, and whether they fit the theoretical framework of Jones and Holmes (1996).

Central to understanding patterns of respiration and nutrient transformations is determining the factors that control these processes in the hyporheic zone (Findlay and Sobczak 2000). A variety of factors can control nitrogen processing; for example, Holmes et al. (1996) showed that denitrification rates beneath a riffle of an Arizona desert stream were raised at the head of a riffle by downwelling labile DOC, and were not inhibited by high DO levels in this zone. In contrast, Hill et al. (1998) found that denitrification in a lowland agricultural stream was limited by the rate of nitrate supply, whereas Duff and Triska (1990) found a negative correlation between denitrification rates and DO along a transect away from a small forest stream. It appears, then, that the factors controlling nitrogen processing differ among stream systems, probably due to differences in nutrient status and quality

and amount of organic carbon. Therefore, it was not obvious which of these factors might control nitrogen processing in the Speed River. Other factors, such as sediment particle size (Jones 1995; Baker et al. 2000; Findlay and Sobczak 2000) and temperature (Pusch 1996), also potentially determine the types and rates of biogeochemical processes. Currently there is strong interest in constructing general and predictive models for the microbial ecology of the hyporheic zone (Findlay and Sobczak 2000), but to achieve this, the relative importance of these various controlling factors must be determined for a variety of stream types. The Speed River, with its particular combination of physicochemical conditions, provided an opportunity to contribute data from a less-studied stream type.

At the reach scale, subsurface hydrology is another important factor exerting control over hyporheic nutrient dynamics. Several recent studies (e.g. Valett et al. 1996; Morrice et al. 1997) have shown that the size of the subsurface storage zone is important in determining the amount of nitrogen retained and transformed within a stream reach. Although the hyporheic zone is not always delimited by a sharp boundary, Fraser and Williams (1998) delimited the hyporheic zone of this Speed River site from the true ground water by discontinuities in physicochemical parameters. They found that the hyporheic boundary, thus defined, shifted with season and therefore altered the size of the hyporheic zone. Since the biogeochemical processes that occur in the hyporheic zone depend on the physicochemical environment (Baker et al. 2000), this raised the question of whether biogeochemical processes also exhibit boundaries that shift with season. If so, this would indicate that hyporheic biogeochemical processes are more important for reach-scale nitrogen dynamics in some seasons than others.

The aims of this study were:

- (1) to determine how microbial nitrification and denitrification change with depth, and between downwelling and upwelling zones, in a moderately N-rich agricultural stream.
- (2) to determine what factors control hyporheic nitrification and denitrification in this stream.
- (3) to determine whether a breakline in these processes could be seen, and shown to shift seasonally with a shifting hyporheic boundary.

Site

The Speed River, southern Ontario, is a gravel bed stream that flows across undulating terrain of glacial till, kame and outwash deposits. The low topographic relief produces a low streambed gradient of 2–5 m per km. The stream lies in a bed of recently deposited alluvium, 1–1.5 m deep and at least 5–10 m wide on each side of the stream. These alluvial deposits have moderately low hydraulic conductivity ($K = \text{approximately } 2 \times 10^{-4} \text{ ms}^{-1}$), but the top 30 cm of the stream bed is composed of coarser materials, primarily gravels (<10 mm) mixed with sands and silts as well as larger cobbles and slabs. Subsurface water flows at the study site

typically are slow; salt tracers released at 40 cm depth take about 20 h to move 25 cm, though in certain places they move the same distance in 10 min.

The sampling site (43°43'54"N, 80°16'24"W), selected to represent typical hydrological and physicochemical conditions in the upper Speed River, is approximately 5 km from the stream's spring source. Upstream of the site approximately 80% of the catchment is in mixed farming, although there are also extensive areas of woodland (Bishop and Hynes 1969). On the south side of the sampling area the land adjacent to the stream is grassland, retired from farming for about 15 years. On the north side is cedar (*Thuja occidentalis*) forest to a distance of more than 100 m, with birch (*Betula papyrifera*) and willow (*Salix* spp.) near the stream. On both sides of the stream to a distance of 10–20 m the stream banks are saturated during wet periods (snow melt to June, September to freeze), and remain moist throughout the year.

At the sampling site, the stream is approximately 6 m wide, varying in depth from about 0.15–0.35 m. In summer, baseflow discharge is $0.1 \text{ m}^3 \text{ s}^{-1}$ (Bishop and Hynes 1969), and in winter this increases by a factor of 2–3.

Materials and methods

Field work

Field work consisted of characterising hyporheic water flow patterns and physicochemical conditions along a single transect, and retrieving hyporheic sediment samples and water from this transect for laboratory 'flow-through' experiments.

Hyporheic sediments, interstitial water samples and hydraulic head measurements were taken along the length of a single 10 m-long riffle. Previous work (Storey 2001) had identified the upstream end of the riffle as a zone of surface water downwelling, particularly during times of low stream flow, and the downstream end as a zone of permanent groundwater upwelling. Hydraulic head contours and subsurface injection of salt tracers had shown that downwelling and upwelling zones were connected by subsurface flow lines (Storey et al. 2003), therefore it appeared that the upwelling zone represented a mixture of surface-derived hyporheic water and true groundwater. Samples were taken from four points along the riffle, spaced about 2.5 m apart; two in the downwelling area (pipes A and B) and two in the upwelling area (pipes C and D). All samples and measurements were collected using a composite sampling device called a 'colonisation corer' (Figure 1). This device consists of a central steel pipe (1.6 m long, internal diameter 4.2 cm) for sampling sediments, surrounded by five smaller pipes or piezometers (internal diameter 1.3 cm) for taking water samples and hydraulic head measurements. The device was driven into the stream bed to a depth of 1.1 m.

Samples were taken on three occasions, spring (April), summer (August) and autumn (November) 2000. The colonisation corer, an artificial substrate sampler, was used in preference to direct sampling methods because it is difficult to extract large sediment samples from the subsurface. Inside the central steel pipe of the colonisation corer was inserted a plexiglas inner sleeve (3.2 cm internal diameter) filled with se-

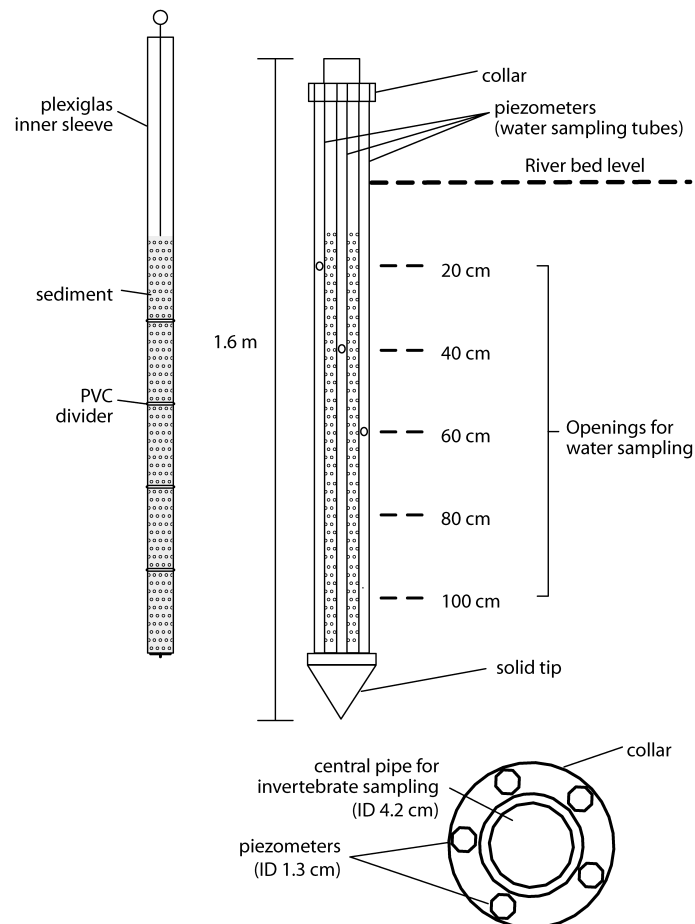


Figure 1. Colonisation corer, showing outer ring of nested piezometers and inner removable plexiglas sleeve.

diment that had been collected from the stream bed surface at the study site. The natural mixture of inorganic and organic particles in the surface sediment was not altered, but the sediment was dried and sieved into a series of grain size fractions. These fractions were then recombined, using different proportions for each section of the inner sleeve, so that at each depth the grain size distribution within the corer matched that of the surrounding sediments, as determined by Stocker and Williams (1972). Particulate organic matter (POM) was significantly higher inside the cores than outside when data from all seasons were combined (paired sample t -test $t = 2.620$, $n = 35$, $p = 0.013$), but in any one season, showed no significant difference between inside and outside. The plexiglas sleeve was divided into five 20 cm-long sections with PVC dividers, so that samples representing depths of 10–30, 30–50, 50–70, 70–90 and 90–110 cm could be separated (for this study, only the upper three sections were used).

Individual samples are referred to in the text as ‘pipe name (depth in centimetres)’, for example, C(60) refers to a sample from pipe C which had a mean depth of 60 cm. Holes (4.5 mm diameter, 100 per 20 cm section) drilled in the sleeve lined up with holes of equal size in the steel corer, allowing through-flow of hyporheic water. With these perforations, the porosity of the colonisation corer was 20%, close to the 25% porosity of the hyporheic sediments. Therefore, although flow rate through the cores was not measured *in situ*, it was assumed that water flow and physicochemical conditions inside the cores were similar to those in the surrounding sediments.

The inner sleeve was left in position for about 24 months before the April sampling, and about 9 weeks before the August and November sampling. Halda-Alija et al. (2001) found 6 weeks sufficient time for hyporheic microflora to colonise a similar device. On retrieval, the sleeves were wrapped in plastic film to limit the sediments’ exposure to oxygen while samples were being processed. Each section of the sleeve was then separated, and held end to end with a glass tube of equal diameter. The sediment column was allowed to slide gently down into the glass tube with minimum disturbance to the sediment structure. The tube was filled with hyporheic water from the same position and depth as the sediment sample, and sealed at both ends with rubber stoppers. Air bubbles were removed by gently tipping/rotating the glass tube and then refilling with water. Sealed samples were kept in a cooler with ice for transport to the laboratory. Two samples of surface sediments also were taken, one from the downwelling and one from the upwelling zone. These were collected by transferring sand and gravel to an enamel tray with a trowel, and from there into a glass tube.

Water samples were taken from the channel and from 20, 40, 60, 80 and 100 cm below the bed surface. Using a peristaltic pump and Tygon™ R3603 tubing, water standing in each piezometer was withdrawn and discarded. A 250 mL sample was taken to measure physicochemical parameters (temperature, conductivity, DO, redox and pH) around each pipe using a Hydrolab H20 multiprobe, then (from the 20, 40 and 60 cm-deep piezometers) a 1.5 L and a 500 mL glass bottle were filled, taking care to avoid air bubbles and minimise exposure of the water to air. The bottles were sealed without bubbles using rubber stoppers, and stored in a cooler until return to the laboratory. Finally, a further 100 mL sample was taken from each piezometer and stored chilled for laboratory determination of nitrate. In the lab this sample was filtered through Gelman™ type A/C glass fibre filters (pore size approximately 1 µm) and analysed within 24 h of collection for NO₃-N ($\pm 0.01 \text{ mgL}^{-1}$), using Hach™ Nitraver 5 powder pillows and the Hach™ DR2000 Spectrophotometer (Hach Company 1992, Loveland Colorado). The result was used to determine how much ¹⁵N-nitrate to add to each perfused core sample. All sample bottles and glassware had been washed in 1:6 HNO₃ and rinsed eight times in distilled water and five times in Nanopure™ deionised water.

Laboratory procedures

A total of 14 sediment and water samples (3 depths × 4 pipes plus 2 surface samples) were used for the flow-through experiments on each date. All experiments

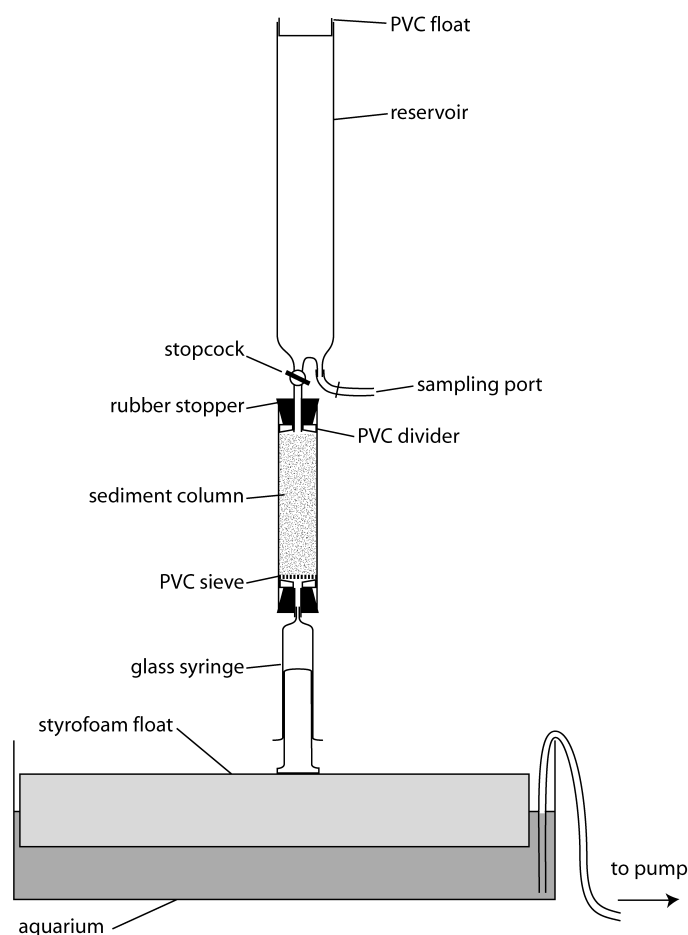


Figure 2. Apparatus used for 'flow-through' experiments. Fourteen such devices were used in parallel.

were conducted in a temperature-controlled room, with the temperature set as near as possible to ambient field conditions (8 °C in April and November, 16 °C in August). The apparatus for the flow-through experiments is shown in Figure 2. Since almost all forms of plastic were found to be permeable to oxygen, glass vessels were used throughout. From each 1.5 L bottle, 350 mL (enough to fill one reservoir) was siphoned into a measuring cylinder, and the remainder was stored in a glass bottle for later refilling of the reservoir. A measured amount of concentrated ^{15}N -nitrate solution was added to the measuring cylinder to increase the nitrate concentration in the sample by about 50%. The sample was stirred with a magnetic stir bar for 1.5 min, then siphoned into the reservoir and sealed with a PVC float.

The amount of sediment in each glass tube was standardised to 10 cm (0.075 L), then a PVC sieve (0.5 mm mesh) was added to the base of each sediment column to prevent fine particles being lost, and the tube was connected to the reservoir above

and a glass syringe below. Reservoir water percolated through the sediment columns under gravity and was collected in the glass syringes beneath. Flow rate through the columns was controlled by limiting the rate at which the plunger in the syringes could fall. This was achieved by resting the plungers on a styrofoam float in an aquarium from which water was pumped at a constant rate. Samples were taken each time 20 mL had collected in the syringes (every 6 h), and the apparatus was reset after returning the pumped water to the aquarium.

The first 200 mL of water in the reservoir was allowed to drip rapidly through the sediment columns, then the flow rate was slowed to 3.3 mL h^{-1} , or 14 mm h^{-1} , for a total travel time of 7 h through the sediment columns. This corresponds to the subsurface flow velocity in the field, as shown by salt tracers. For the first 12 h water collecting in the syringes was discarded, then the reservoirs were refilled with ^{15}N -nitrate-amended water and the first samples from the reservoir were taken. Parameters measured in the flow-through experiment were DO (3–4 replicates), Fe^{2+} (2 replicates, November only), nitrate, nitrite, ammonium, DOC and denitrification (2 replicates each). Each parameter was measured first in the reservoir, then in the next syringe sample, 6 h later, so that ‘initial’ and ‘final’ samples were taken as nearly as possible from the same ‘packet’ of water. Replicates of each parameter were interspersed with replicates of the other parameters to ensure that any gradual changes over time in any one parameter were recorded.

After all parameters had been measured, the reservoirs were refilled with ^{15}N -nitrate-amended water that had the nitrification inhibitor nitrapyrin (2-chloro-6-trichloromethyl-pyridine) added to a final concentration of $15 \mu\text{M}$ ($40 \mu\text{M}$ in November), then the same parameters were measured again. The nitrapyrin solution had been made by dissolving nitrapyrin crystals in distilled water, heated to about 60°C and stirred for several hours. In August, the crystals were first dissolved in a small amount of ethanol (concentration not more than 5% in the final solution). Following the nitrification-inhibited run, the flow-through procedure was repeated a third time with ^{15}N -nitrate- and nitrapyrin-amended water that had been shaken vigorously to achieve oxygen saturation. The entire process took 8 days.

Oxygen was measured using a Hydrolab H20 polarographic electrode (precision $\pm 0.1 \text{ mg L}^{-1}$), Fe^{2+} and ammonium using the Hach 1,10 phenanthroline and Nessler methods, respectively (precision $\pm 0.01 \text{ mg L}^{-1}$ and $\pm 0.01 \text{ mg L}^{-1}$, respectively), and nitrate and nitrite using ion chromatography (precision $\pm 0.02 \text{ mg L}^{-1}$ and $\pm 0.005 \text{ mg L}^{-1}$ respectively).

Denitrification was measured using the isotope pairing procedure of Nielsen (1992); syringe samples containing dissolved nitrogen gas were injected gently into 18 mL glass vials and immediately capped with butyl rubber stoppers. Then 3.4 mL of water was withdrawn through a syringe needle and replaced with high purity helium gas. After vigorous shaking to equilibrate dissolved gases with the headspace, 1 mL of headspace was withdrawn in a gas-tight syringe and injected into a mass spectrometer (Isochrom Continuous Flow Stable Isotope Mass Spectrometer coupled to a Carla Erba Elemental Analyser; CHNS-O EA1108).

Denitrifying bacteria combine ^{15}N and ^{14}N from added and naturally-occurring nitrate, according to the proportions available, to produce $^{15}\text{N}^{14}\text{N}$ and $^{15}\text{N}^{15}\text{N}$ gas.

The rate of total denitrification is the sum of the denitrification rate of added ^{15}N -nitrate (D_{15}) and the denitrification rate of naturally-occurring ^{14}N -nitrate (D_{14}). Both of these values were calculated from the amounts of $^{15}\text{N}^{14}\text{N}$ and $^{15}\text{N}^{15}\text{N}$ above natural levels in the headspace. According to Nielsen (1992), D_{15} is simply the sum of ^{15}N in the produced labelled dinitrogen:

$$D_{15} = (^{15}\text{N}^{14}\text{N}) + 2(^{15}\text{N}^{15}\text{N})$$

D_{14} was then calculated from D_{15} :

$$D_{14} = D_{15} \frac{f_{14}}{f_{15}}$$

where f_{14} and f_{15} are the frequencies of ^{15}N -nitrate and ^{14}N -nitrate in the water. The ratio of f_{14}/f_{15} was calculated from the amounts of excess $^{15}\text{N}^{14}\text{N}$ and $^{15}\text{N}^{15}\text{N}$ in the headspace:

$$\frac{f_{14}}{f_{15}} = \frac{\text{N}^{14}\text{N}}{2(^{15}\text{N}^{14}\text{N})}$$

Total denitrification (D_{total} ; nmol) from the sample is then simply $D_{14} + D_{15}$. This figure was converted to nanogram $\text{NO}_3\text{-N}$ consumed per g sediment per hour:

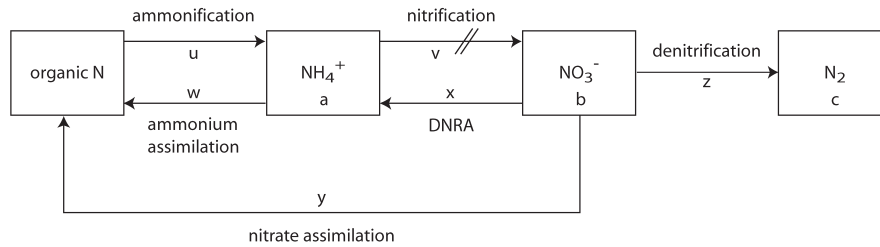
$$\text{ng NO}_3\text{-N g sediment}^{-1}\text{h}^{-1} = \frac{(D_{\text{total}} 14 \times 3.4)/(dv) 3.3}{m}$$

where 14 is the atomic mass of nitrogen, 3.4 is the total headspace volume in the vial, d is the distribution coefficient of nitrogen gas between headspace and water, v is the volume of water in the glass vial, 3.3 is the flow rate of water through the cores (mL h^{-1}), and m is the mass of the sediment core.

At the end of the flow-through procedure, sediment samples were removed from the glass tubes and placed in saturated CaCl_2 solution to separate the organic from inorganic particles. POM was quantified by the weight loss on ignition method (Nelson and Sommers 1996): samples were dried at 105°C for 24 h, weighed, combusted at 400°C for 14 h and reweighed. Finally, the size distribution of inorganic particles was determined by passing the sediments through a sieve series and weighing the fractions. The percentage of particles less than $210\text{ }\mu\text{m}$ was used as a proxy measure of surface area available for biofilm growth.

Analyses

Physicochemical parameters measured in the field were used to divide the transect into a more surface water-influenced and a more groundwater-influenced zone for each season. This was achieved by cluster analysis (K -means clustering with 2 means) of the full set of physicochemical parameters (temperature, DO, conductivity, redox and pH), using the SPSS for Windows (version 10, SPSS Inc., Chicago) statistical software. The same software was used for analysis of the flow-



If a_1 = rate of change in NH_4^+ in first run (no nitrification inhibitor) $\text{ng N} \cdot \text{g sediment}^{-1} \cdot \text{h}^{-1}$
 a_2 = rate of change in NH_4^+ in second run (with nitrification inhibitor) $\text{ng N} \cdot \text{g sediment}^{-1} \cdot \text{h}^{-1}$

$$\begin{array}{lll} \text{Then } a_1 = u_1 - w_1 - v_1 + x_1 & a_2 = u_2 - w_2 + x_2 & \text{Assuming } y_1 = y_2, x_1 = x_2: \\ b_1 = v_1 - x_1 - y_1 - z_1 & b_2 = -x_2 - y_2 - z_2 & v_1 = (b_1 + z_1) - (b_2 + z_2) \quad (1) \\ c_1 = z_1 & c_2 = z_2 & \end{array}$$

$$\begin{array}{l} \text{If } x_2 = 0: \\ x_1 - v_1 = (b_2 + z_2) - (b_1 - z_1) \quad (2) \end{array}$$

Figure 3. Parts of the nitrogen cycle that occur in hyporheic sediments. Boxes refer to pools of the different nitrogen species, and the letter symbol inside refers to the rate of change of the N species in that box: (concentration after – concentration before)/mass of sediment/duration of flow-through. Letter symbols by the arrows refer to the rate of the corresponding N-transforming process. Rates of the various N-transforming processes can be calculated from rates of changes in the various N pools using the equations given. Subscript 1 refers to the rate without any added nitrification inhibitor; subscript 2 refers to the rate with inhibitor. ‘DNRA’ refers to dissimilatory nitrate reduction to ammonium.

through results, with t-tests to compare downwelling and upwelling zones, one-way ANOVA to compare different pipes, and Pearson’s r as a basis for testing correlations between parameters.

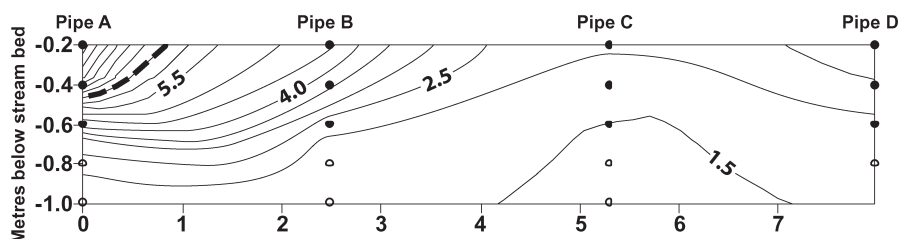
Rates of nitrogen-transforming processes were quantified using the scheme and equations shown in Figure 3. This scheme shows how concentrations of ammonium, nitrate and dissolved nitrogen gas in hyporheic water before and after it has percolated through hyporheic sediments can be used to quantify rates of nitrification, denitrification and ammonification of organic nitrogen, using the equations shown. Because more than one process acts simultaneously on the ammonium and nitrate pools, nitrification can not be quantified by a single measurement of the changes in ammonium and nitrate. Therefore a nitrification inhibitor was added after the first set of measurements, and changes in the nitrate and ammonium pools measured a second time. By comparing this second set of measurements to the first, nitrification could be measured – Equation (1) in Figure 3.

Results

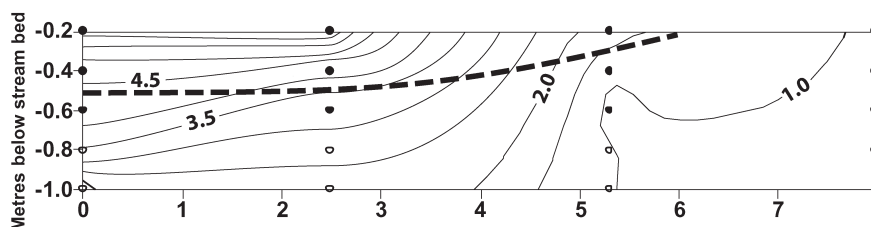
Field patterns

DO was selected as the clearest indicator of surface water intrusion. In all seasons, DO showed clear gradients (Figure 4); subsurface oxygen values were higher in

a) April Surface water = 10.9-12.5 mgL⁻¹



b) August Surface water = 8.4-8.7 mgL⁻¹



c) November Surface water = 10.2 mgL⁻¹

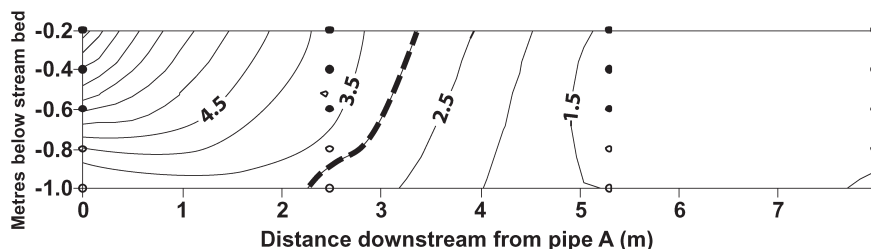


Figure 4. Contour plots of dissolved oxygen (DO) along the transect; contour lines are at 0.5 mg L⁻¹ intervals. Circles indicate the positions of actual sample points, that is, the openings of piezometers. Water and sediments for lab experiments were taken from the top 60 cm, that is, the filled circles. The dashed line separates the two groups determined by cluster analysis. The vertical axis is exaggerated by a factor of 2.

shallower than in deeper samples, and in upstream, downwelling pipes (A and B) than in downstream, upwelling pipes (C and D). In April, only A(20) and A(40) had high DO concentrations, indicating that pipe A was the main point of downwelling, and that rapid oxygen uptake and/or dilution with groundwater occurred over a flow path of 60 cm. Pipe B showed oxygen concentrations above those in pipes C and D,

and a definite depth gradient, indicating some surface water influence. At pipes C and D, oxygen concentrations were less than 2 mg L^{-1} with almost no depth gradient, indicating either that surface-derived hyporheic water reaching these pipes had been depleted of almost all oxygen, or that interstitial water here was almost entirely of groundwater origin.

In August, high DO concentrations were found in A(20) and B(20), indicating downwelling at both pipes. Concentrations declined slightly more rapidly with depth in B than A, but values were similar in both pipes. As in April, pipes C and D showed very low DO, even at 20 cm, suggesting strong upwelling at C. In November, oxygen levels were highest at A(20), and as in April there was a decline in oxygen between pipes A and B; the concentration in B(20) was as low as in A(80), but pipe B was still distinctly higher than pipes C and D, which were uniformly low.

Patterns in the other physicochemical parameters (temperature, conductivity, redox and pH) were similar to, but more variable than, oxygen. All of these parameters were combined in a cluster analysis to divide the samples into two groups (Figure 4). The breaklines show that the influence of surface water was restricted to a small area in April, occurred shallowly but over a wider area in August, and extended more deeply in November. Hydraulic head data (not shown) confirmed that upwelling hydraulic gradients were strongest in April, and declined steadily towards November. They also confirmed that towards November, downwelling and upwelling zones became more clearly differentiated in terms of vertical hydraulic gradient.

Nitrate profiles were very similar to those of oxygen. Nitrate typically was higher in surface than hyporheic water, and decreased with depth and distance along the flow line; in November, the concentration in the surface water was $0.28\text{--}0.3 \text{ mg L}^{-1}$, decreasing during flow through the hyporheic zone to 0.02 mg L^{-1} at pipe C.

Flow-through

Results from November only are presented here, as these represent the most complete dataset, and were similar to the results from August. Results from August and April are presented in the section 'Seasonal differences' at the end.

Initial DO levels showed a distinct break between downwelling zone (pipe A and B) cores and upwelling zone (pipe C and D) cores, with a correlation between oxygen and depth among the downwelling zone cores (Pearson's $r = -0.848$, $n = 17$, $p < 0.001$) but not among the upwelling cores (Figure 5(a)). This corresponded to the breakline shown in the field data (Figure 4(c)). Aerobic respiration in all subsurface cores was rapid enough that oxygen levels were reduced to just above 2 mg L^{-1} in all cores, regardless of the initial level; only the two surface cores failed to reduce oxygen to this level. This 2 mg L^{-1} , however, is likely to be an overestimate of the true DO concentrations, a result of not calibrating the meter to zero during the experiment. The fact that in many of the cores oxygen concentrations were reduced to this same base level, yet significant Fe^{2+} was produced

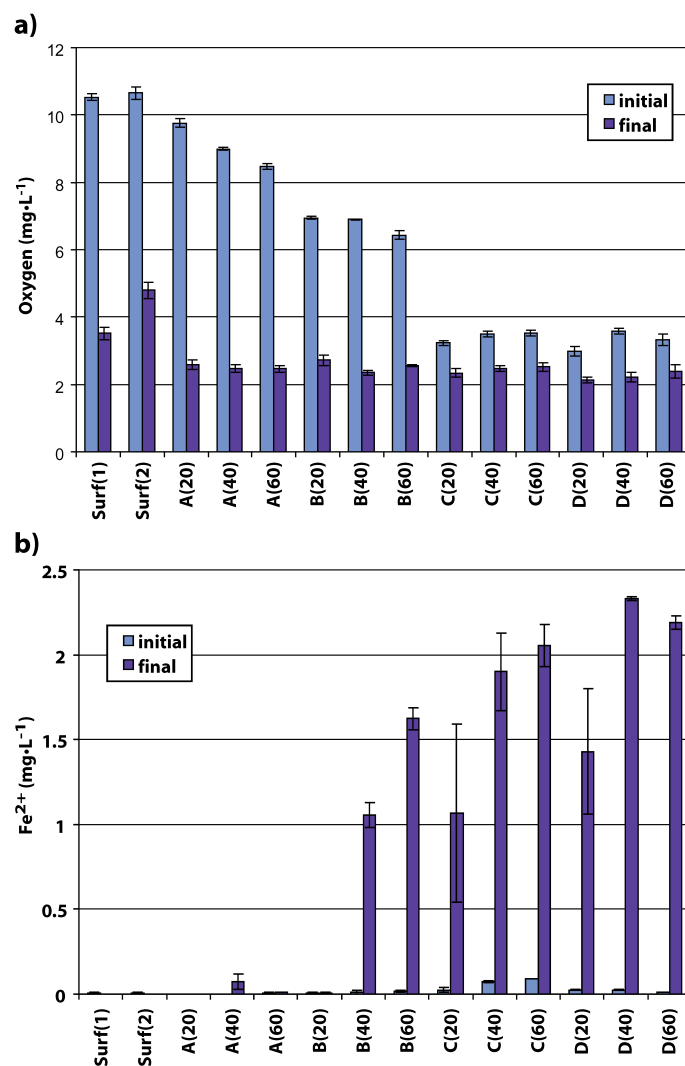


Figure 5. (a) Initial (reservoir) and final (syringe) concentrations of DO from the 14 sediment cores of the flow-through experiment (± 1 standard error; 3 replicates) in November; (b) Initial and final concentrations of Fe²⁺ (± 1 standard error; 2 replicates) in November.

in several of the cores (see below) suggests that true oxygen concentrations were lower than 2 mg L^{-1} . Also, a different meter used in April measured DO as low as 0.4 mg L^{-1} , suggesting November values should have been at least as low. However, the meter used in November was able to read as low as 1.4 mg L^{-1} during the nitrification-inhibited runs, showing that the readings of 2 mg L^{-1} at least were higher than the minimum detectable. Because of their high initial oxygen, actual

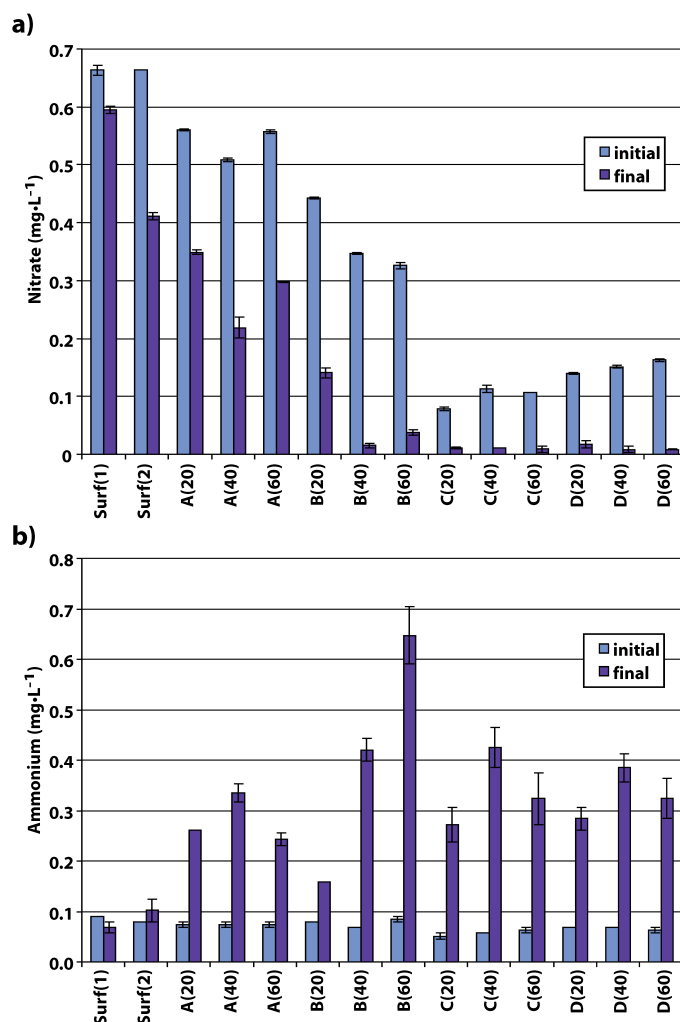


Figure 6. Initial and final concentrations of (a) nitrate; and (b) ammonium (± 1 standard error; 2 replicates each) in November.

aerobic respiration rates were highest in the downwelling (pipe A and B) and surface cores.

Redox conditions in the cores were indicated by the evolution of Fe^{2+} (Figure 5(b)). Fe^{2+} clearly separated the cores into two groups, the shallow, downwelling cores with redox potential above about 150 mV, and the deeper or upwelling cores, with redox potential below about 150 mV. A sharp breakline occurred between B(20) and B(40).

Initial nitrate levels (Figure 6(a)) showed a pattern similar to DO. Surface and downwelling zone sediments removed a greater amount of nitrate than the

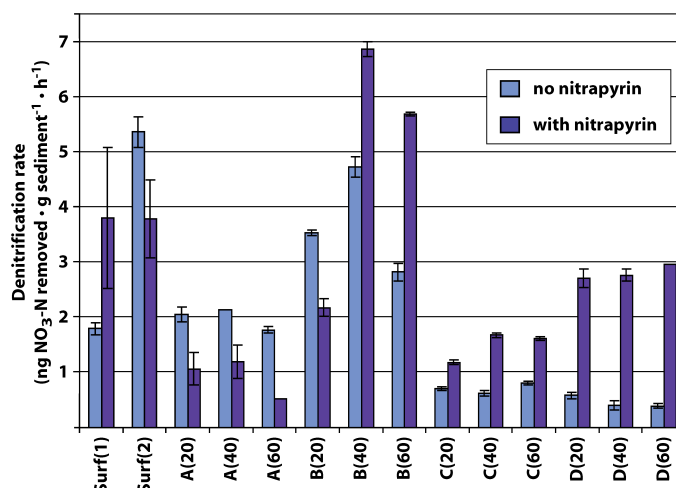


Figure 7. Denitrification rates in the 14 sediment cores (± 1 standard error; 2 replicates) in November, without and with the nitrification inhibitor nitrapyrin.

upwelling zone ($t = 4.294$, $n = 28$, $p < 0.001$; 2-tailed, unequal variances assumed), but cores B(40) to D(60) reduced nitrate concentrations to almost zero. B(40) and B(60) were unusual in reducing large initial concentrations to almost zero. In contrast, initial ammonium levels were uniformly low, and concentrations increased greatly during flow through all cores, except at the surface, where final concentrations were not significantly higher than initial ($t = 0.00$, $n = 8$, $p = 1.00$; Figure 6(b)). Upwelling zone cores produced slightly higher final ammonium concentrations than downwelling cores, but the difference was significant only if B(40) and B(60) were excluded, or were included with the upwelling cores ($t = 2.198$, $n = 24$, $p = 0.039$; 2-tailed, unequal variance). Denitrification was significantly higher in downwelling zone than upwelling zone cores ($t = 6.752$, $n = 28$, $p < 0.001$; 2-tailed, unequal variance; Figure 7). Unexpectedly, the highest rate of denitrification occurred in surf(2), that is, surface sediments from the upwelling zone, although in surf(1) denitrification rates were no higher than in downwelling zone sediments.

POM within the cores is shown in Figure 8. POM content in November did not differ significantly between the different pipes ($F = 0.134$; $df = 3, 8$; $p = 0.937$), but showed a definite increase with depth in each pipe (Pearson correlation $r = 0.927$, $n = 12$, $p < 0.001$). This contrasts with the POM content of the surrounding sediments, which showed no consistent change with depth (Pearson $r = -0.338$, $n = 12$, $p = 0.283$). Overall, in November there was no significant difference in amount of POM between the cores and the surrounding sediments (paired sample t -test $t = 1.225$, $n = 12$, $p = 0.246$).

Addition of the nitrification inhibitor nitrapyrin produced unexpected effects. Whereas final oxygen concentrations were expected to be higher than in the

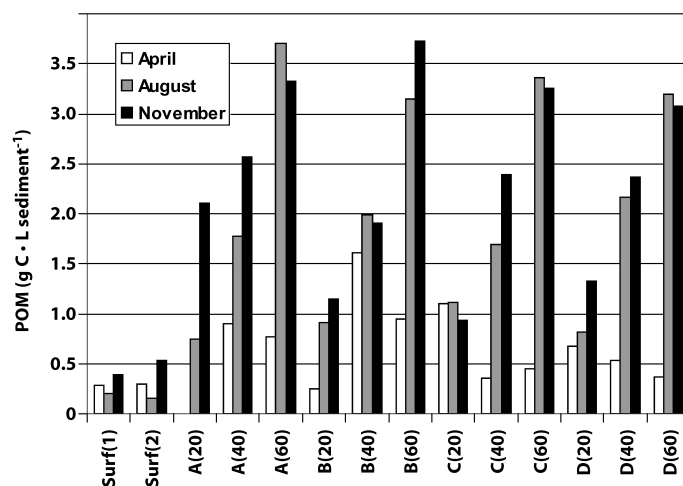


Figure 8. POM content of the flow-through cores in three seasons (1 replicate each).

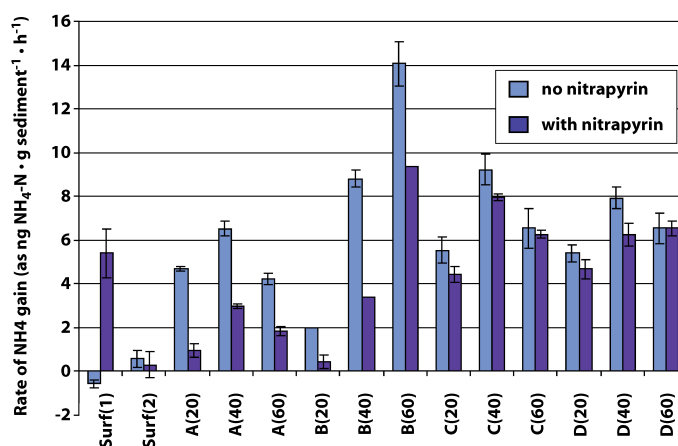


Figure 9. Rates of ammonium gain (± 1 standard error) in November, without and with the nitrification inhibitor nitrapyrin.

previous run due to the inhibition of oxygen-consuming nitrification, in fact final concentrations were slightly lower in all cores, except A(20) which showed a very slight increase. Ammonium concentrations were expected to increase by a greater amount in all cores after addition of nitrapyrin (a_2 in Figure 3), since an ammonium-consuming process (v) was inhibited, but in fact in all cores except surf(1) and D(60) there was less increase in ammonium with nitrapyrin than without (Figure 9). Similarly, nitrate losses were expected to increase in all cores after addition of nitrapyrin (b_2 in Figure 3), since a nitrate-producing process (v) was

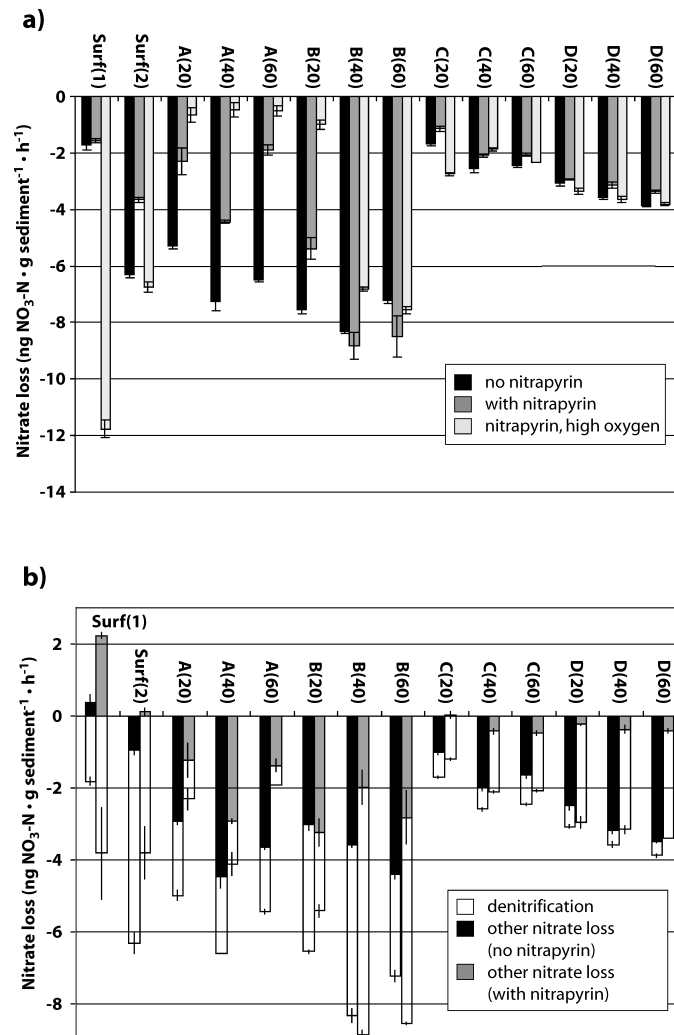


Figure 10. (a) Rates of nitrate loss (± 1 standard error) in November: without nitrapyrin; with nitrapyrin; and with nitrapyrin and reservoir water saturated with oxygen. (b) Rates of nitrate loss (± 1 standard error) in November: without nitrapyrin; with nitrapyrin. For each core, the proportion of nitrate loss not accounted for by denitrification is highlighted by shading.

blocked, but in fact in all cores except B(40) and B(60) there was less nitrate loss (Figure 10(a)). Finally, denitrification was expected to be lower in the presence of nitrapyrin, since the supply of nitrate should have been reduced, but in fact denitrification was considerably higher in B(40, 60) and the upwelling cores; the lower denitrification in surf(2) and the downwelling cores A(20) to B(20) (Figure 7) was

associated with higher, not lower, available nitrate, which suggests it was due to a direct inhibitory effect of nitrapyrin in these aerobic cores.

These results led to the conclusion that the rate of nitrification (v in Figure 3) was insignificant in all cores compared to the rate of the opposite process, dissimilatory nitrate reduction to ammonium (DNRA; x in Figure 3), and that DNRA also was blocked by nitrapyrin. Evidence to support these conclusions is that in the upwelling cores the rate of nitrate loss decreased after addition of nitrapyrin although the denitrification rate increased. Figure 10(b) shows total nitrate loss in each core, and the proportion not accounted for by denitrification, before and after addition of nitrapyrin. Before the nitrapyrin addition, there was considerable nitrate loss that was not accounted for by denitrification, yet in the presence of nitrapyrin this amount dropped to almost zero in cores C(20) to D(60).

Based on these conclusions, and using the equations from Figure 3, rates of net DNRA (i.e., DNRA minus nitrification) could be calculated. Assuming that nitrate assimilation does not change significantly after addition of nitrapyrin (which we verified), net DNRA is the difference in non-denitrification loss of nitrate before and after addition of nitrapyrin; $(b_2 + z_2) - (b_1 + z_1)$ from Equation (2) in Figure 3. Net DNRA rates were highest in the pipe D cores (average $2.8 \text{ ng NO}_3\text{-N g sediment}^{-1} \text{ h}^{-1}$) and lowest in pipe C (average $1.3 \text{ ng NO}_3\text{-N g sediment}^{-1} \text{ h}^{-1}$), whereas the pipe A and B and surface cores in general had intermediate rates. Large standard errors, however, made most of these differences insignificant. The distribution of net DNRA rates did not appear to be strongly related to the pattern of any other parameter measured. Nitrite, which might be expected to accumulate during DNRA, was detectable only in surf(1), A(20,40 and 60) and B(20), reaching a maximum concentration of 0.04 mg L^{-1} in A(60) and B(20).

Figure 11 summarises the fluxes of nitrogen through the downwelling zone (core A, averaged across the 3 depths) and the upwelling zone (core D, also averaged across the 3 depths) according to the scheme originally described in Figure 3.

Controlling factors

Just as the rates of various processes were very different between the two groups of cores, surf(1) to B(20) and B(40) to D(60), the factors limiting these processes also were different between these two groups. Denitrification and DNRA appeared to be limited by oxygen among cores surf(1) to B(20), where initial oxygen concentrations were $10.5\text{--}6.9 \text{ mg L}^{-1}$, but not in the upwelling group and B(40,60), where initial oxygen concentrations were $6.5\text{--}3.2 \text{ mg L}^{-1}$; evidence is first that when reservoir water was saturated with oxygen, the downwelling group showed a large drop in nitrate loss whereas the upwelling group actually showed an increase (Figure 10(a)). Second, at natural concentrations of oxygen, total nitrate loss was correlated with oxygen concentration within the downwelling group (cores surf(1) to B(60); $r = -0.711$, $\text{df} = 6$, $p = 0.048$) but not within the upwelling group ($r = 0.102$, $\text{df} = 4$, $p = 0.848$).

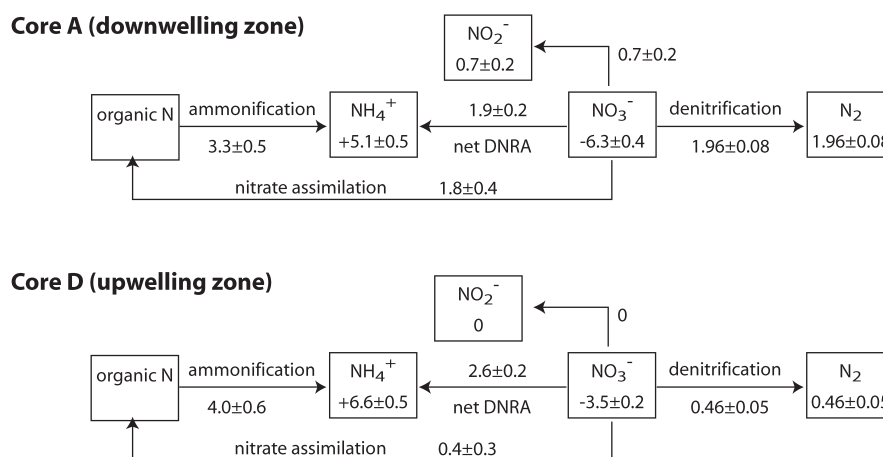


Figure 11. Summary of nitrogen fluxes through downwelling zone core A (averaged from 20, 40 and 60 cm deep) and upwelling zone core D (also averaged from 20, 40 and 60 cm deep) in November. Units for all values are $\text{ng N g sediment}^{-1} \text{h}^{-1}$. Boxes represent pools of the various nitrogen species, arrows represent processes.

In the upwelling group, denitrification and DNRA appeared to be limited by nitrate (Figure 12(a–d)), which occurred at much lower concentrations in this group than in the downwelling group. Comparison of Figure 12(a), (b), (c) and (d) suggests that DNRA outcompeted denitrification for nitrate in the upwelling group. Before addition of nitrapyrin, when both processes were able to proceed, DNRA showed a strong positive correlation with available nitrate ($r = 0.96$, $\text{df} = 4$, $p < 0.01$) whereas denitrification did not ($r = -0.86$, $\text{df} = 4$, $p = 0.03$). However, once DNRA was inhibited by nitrapyrin, denitrification showed a strong positive correlation with available nitrate ($r = 0.99$, $\text{df} = 4$, $r < 0.01$). The downwelling group showed a negative correlation with available nitrate in Figure 12(a and d) because nitrate and oxygen were strongly correlated within this group ($r = 0.90$, $\text{df} = 6$, $p < 0.01$).

Other factors that may have limited rates of denitrification and DNRA, such as energy supply and available surface area for biofilm growth, appeared to have less effect. DOC, measured only in April and August, increased slightly in most cores but decreased slightly in some, and changes could not be correlated with any other processes. POM showed a weak correlation with ammonium increase among all cores without nitrapyrin ($r = 0.76$, $\text{df} = 12$, $p < 0.01$; cf. $r = 0.46$, $\text{df} = 12$, $p > 0.05$ with nitrapyrin), implying it had some effect on DNRA. Percentage of sediment particles less than $210 \mu\text{m}$, a proxy measure of surface area available for biofilm growth, also was correlated with ammonium increase ($r = 0.74$, $\text{df} = 12$, $p < 0.01$), but this may be due only to its strong correlation with POM ($r = 0.94$, $\text{df} = 12$, $p < 0.001$). Both POM and sediment particle size were correlated with evolution of Fe^{2+} among cores C(20) to D(60) ($r = 0.91$, $\text{df} = 4$, $p = 0.01$; $r = 0.83$, $\text{df} = 4$,

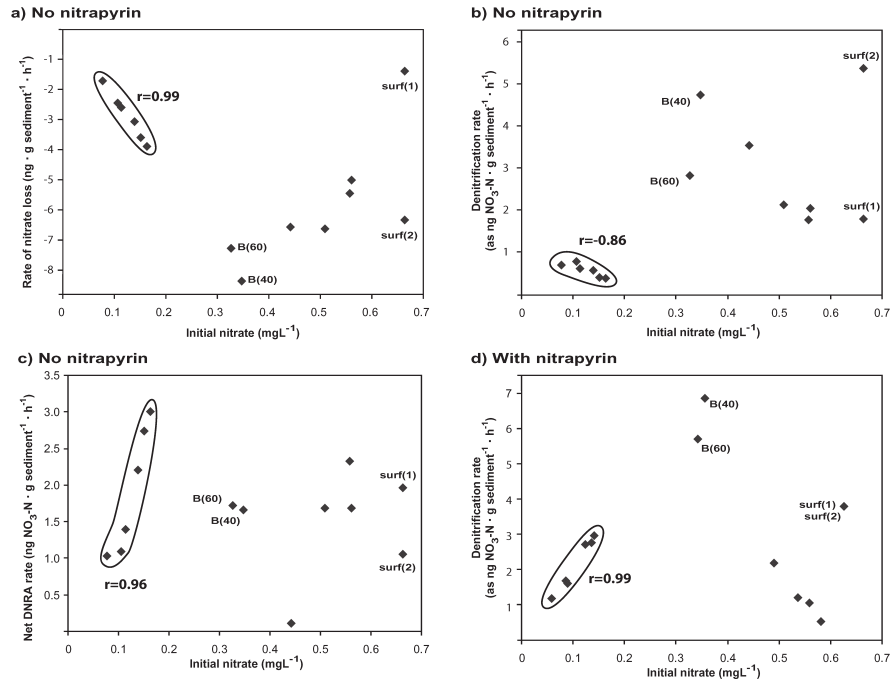


Figure 12. Nitrate limitation of denitrification and DNRA in November. Total nitrate loss is presumed to be the sum of denitrification and DNRA. Net DNRA means DNRA minus nitrification.

$p = 0.041$, respectively) suggesting they may have indirectly influenced N-processing by affecting redox potential in the upwelling cores.

Seasonal differences

Oxygen and nitrogen changes in August overall were similar to changes in November, but included some important differences. Initial oxygen levels in all cores were lower, typically by 1–2 mgL⁻¹, in August than in November. Final oxygen concentrations were reduced to the same base level of 2 mgL⁻¹ in all cores, and when initial oxygen concentrations were raised to saturation, all cores except A(20) and B(20) continued to reduce final oxygen concentrations to this level. Therefore, as might be expected given that experimental conditions were 8 °C warmer in August than in November, respiration appeared to be more rapid in August, and oxygen was probably depleted earlier along the interstitial flow path. Associated with this, total nitrate loss in August showed no correlation with initial oxygen level among the downwelling cores (Pearson's $r = -0.478$, $n = 8$, $p = 0.231$) and denitrification in fact showed a positive correlation, caused by the surface cores which had high oxygen and denitrification rates. This implies that denitrification in these

cores was not inhibited by oxygen. Only A(20) showed a low denitrification rate that was probably the result of oxygen inhibition. Among all cores except A(20), denitrification was positively correlated with initial nitrate (Pearson's $r=0.824$, $n=13$, $p=0.001$), indicating that it was nitrate-limited in all except the shallowest downwelling cores.

In April, patterns of oxygen and nitrogen changes were quite different from those in August and November. In April, initial oxygen concentrations were not significantly different to those in November (paired sample t -test $t=0.762$, $n=12$, $p=0.462$), and the temperature was similar, but aerobic respiration appeared lower overall; final oxygen concentrations were reduced to what appeared to be a base level only in B(60) and C(20–60), whereas in cores A(40, 60) and B(20), final oxygen concentrations were as high as $4.5\text{--}7\text{ mg L}^{-1}$. The surface core, however, showed a similar respiration rate to surface cores in November ($1.35\text{ mg L}^{-1}\text{ h}^{-1}$ cf. average of $1.07\text{ mg L}^{-1}\text{ h}^{-1}$). Initial nitrate concentrations were not significantly different to those in November (paired sample t -test $t=0.044$, $n=12$, $p=0.965$), but in April, final nitrate concentrations were higher than initial in all cores, suggesting that in all cores nitrification was significantly higher than DNRA. Associated with this, ammonium concentrations increased very little during flow through the cores in April (compared to an average 14 times greater increase in November). Denitrification rates in April were not significantly different to rates in November (paired sample t -test $t=1.104$, $n=12$, $p=0.293$), but denitrification was undetectable in A(40,60) and B(20), probably due to the high oxygen in these cores. POM was much lower in almost all the subsurface cores in April, generally 50–75% lower than in August and November, although the April surface core contained a similar amount of POM to the August and November surface cores.

Discussion

The results of the flow through experiments differed from expectations in several ways. In particular, the effects of the nitrification inhibitor, nitrapyrin, on the nitrate and ammonium pools were opposite to expectations, leading to the conclusions that DNRA was occurring in all the cores, and that it was blocked by nitrapyrin. Except in a few rare cases (e.g., Kelso et al. 1999), the occurrence of DNRA in riverine sediments has not been documented as it is generally assumed to be insignificant compared with denitrification (Duff and Triska 2000). This is likely true in many, or most, stream systems, since more energy can be gained from reduction of nitrate to dinitrogen than from reduction to ammonium (Tiedje 1988). However in situations where electron donors are abundant relative to electron acceptors, DNRA is favoured over denitrification as it is a more efficient pathway for removing electrons (Tiedje 1988). This situation may occur where carbon is abundant and nitrate in short supply, as was the case in the streams studied by Kelso et al. (1999), and as appeared to be the case in cores from this Speed River site. Although DOC is not much higher in the Speed River than in other sites where hyporheic nutrient dynamics have been studied (e.g., Triska et al. 1993; Jones et al. 1995; Valett et al.

1996), POM in the cores we collected was at least three times higher than reported from most other sites (Pusch and Schwoerbel 1994; Jones 1995; Naegeli and Uehlinger 1997).

Inhibition of DNRA by nitrapyrin has not been reported in any studies we have found, but the mechanism by which nitrapyrin acts is complicated (Vannelli and Hooper 1992), and inhibition of other processes, such as denitrification, methanogenesis, sulphate reduction (Vannelli and Hooper 1993) and ammonification of organic nitrogen (Malhi and Nyborg 1983) have been reported. We also inferred that nitrapyrin partially inhibited denitrification in the more aerobic cores but not in the less aerobic ones. This differential effect on denitrification has not been reported either, but nitrapyrin is known to react differently within cells in aerobic vs. anaerobic environments (Vannelli and Hooper 1993), so we believe that this is a plausible interpretation of our data.

Spatial patterns and controlling factors in nitrogen-transforming processes

Patterns in denitrification were not as expected, but showed similarities to some other published studies. Though an anaerobic process, denitrification occurred at higher rates in the more oxic surface and downwelling zone cores. This was almost certainly due to the higher nitrate in the downwelling zone, as denitrification was strongly correlated with nitrate concentration among the upwelling zone cores. Hill et al. (1998) reported that denitrification rates in another N-rich agricultural stream similarly were limited by the rate of nitrate supply. Organic carbon, which appeared to be responsible for raising the denitrification rate of the downwelling zone above that of the upwelling zone in an Arizona desert stream (Holmes et al. 1996), did not seem to be an important factor in the Speed River. DOC, though it was higher in the downwelling zone, did not appear to be actively taken up in the cores, and POM did not show any difference between downwelling and upwelling zone cores.

Denitrification rates usually are negatively correlated with oxygen in field studies (e.g., Triska et al. 1993), however several studies have reported denitrification occurring in aerobic sediments (e.g., Nakajima 1979; Ventullo and Rowe 1982; Holmes et al. 1996; Schramm et al. 1996). Since denitrification among most bacteria is inhibited by oxygen concentrations above 0.3 mg L^{-1} (Tiedje 1988), hyporheic studies have all concluded that denitrification must be occurring in small pockets of anoxic sediments, which may form in low permeability sediments where water turnover is low (Baker et al. 2000), or in deposits of POM where respiration is high (Duff and Triska 1990). The cores in our flow-through study, however, were only $3.1 \text{ cm diameter} \times 10 \text{ cm}$ long and contained sieved, standardised sediment, thus it is unlikely that anoxic pockets occurred within the oxic cores. A more likely explanation for the occurrence of denitrification within these cores is that the micrometres-thick biofilm, within which almost all hyporheic bacteria exist, acts an effective barrier to limit the diffusion of oxygen to bacterial cells. Models (Riemer and Harremoës 1978) and *in situ* measurements from aerobic trickling filters (Schramm et al. 1996) have shown that aerobic respiration in the outer layers of bacterial biofilms can produce anoxic conditions in the

inner layers that allow denitrification, despite oxic conditions in the overlying water. Biofilms in trickling filters likely show higher respiration rates than hyporheic biofilms, but the same microgradients of oxygen have been shown within biofilms on the surface of natural stream beds (Sabater et al. 2002), so it would not be surprising to find them also within hyporheic biofilms. The concentration of oxygen in the bulk water, however, still affects the concentration at the base of the biofilm, as it determines the diffusion gradient. This explains why, in our study, denitrification among the downwelling zone cores was negatively correlated with oxygen in November, and in April was undetectable in several cores which had oxygen concentrations of $4.5\text{--}7\text{ mg L}^{-1}$.

Denitrification in this Speed River site, therefore, was controlled primarily by nitrate availability and secondarily by oxygen inhibition. Organic carbon was probably in excess, so did not limit denitrification, sediment particle size showed no significant effect, and comparison of rates between seasons suggested that temperature was of minor importance (cf. Jones 1995; Holmes et al. 1996). DNRA appeared to be controlled by the same factors, though POM and/or sediment particle size appeared to exert a weak influence on DNRA.

Nitrification was impossible to quantify separately from the reverse process, DNRA, in this study, but the relative rates of nitrification, DNRA and denitrification could be determined by the gain or loss of nitrate during flow through the cores. In August and November, nitrate decreased, indicating that nitrification rate was low compared with DNRA and denitrification. The most likely reason is that the high amount of POM in these cores not only favoured DNRA, but also allowed heterotrophs to outcompete nitrifiers for oxygen (Schramm et al. 1996). This explanation is supported by contrasting the April data. In April, nitrate increased in all cores, indicating that nitrification was more rapid than DNRA. Associated with this, respiration was much lower in April than in November, hence oxygen levels were higher. The most likely reason that respiration was much lower in April is that April cores had 50–75% less POM than November cores. Therefore we suggest that POM had a negative effect on nitrification rate in this study.

Relationship to field patterns

In terms of DO and nitrate, changes measured in the flow-through experiments corresponded to physicochemical patterns observed in the field; both DO and nitrate declined within sediment cores and along hyporheic flow lines. Rates of these changes, however, were generally higher in the flow-through experiments. In cores from the downwelling zone, DO was reduced by $6\text{--}7\text{ mg L}^{-1}$ over a 10 cm flow path, whereas in the field, a flow path of more than 1 m was required for the same drop in DO. A similar relationship was found for nitrate loss. One explanation is that POM in the cores was fresher, and hence more labile, than POM occurring naturally in the hyporheic sediments, even though total POM, measured as ash-free dry mass, was comparable inside and outside the cores. POM had not been inserted into the cores in a deliberate way, but was simply a component of the surface-derived fill for the cores. Thus the POM in the cores probably was exposed to a

shorter decomposition period than POM buried naturally in the hyporheic sediments. Another possible explanation is that during handling and transport of the cores, the POM particles inside were reoriented and microbial processing was stimulated. Finally, the longer flow paths in the field may be partly due to the heterogeneity of the stream bed sediments, preferential channels in the subsurface allowing some of the hyporheic water to travel faster than the measured average rate.

With respect to nitrate, the rate of loss may have been slightly elevated in the cores due to the addition of the ^{15}N tracer, which raised nitrate levels by about 50%. Since denitrification appeared to be nitrate-limited, it may have proceeded slightly faster in the cores than in the field at these dates. However, the rate of denitrification should not have been unnaturally high; nitrate levels in the Speed River vary naturally over time, and even with the addition of the tracer, nitrate levels in the cores were within the range of levels previously measured in the field. Other nitrogen processes are unlikely to have been affected significantly by the nitrate tracer addition. Nitrification rates clearly were not raised, and since DNRA is generally favoured by a high ratio of organic carbon to nitrate (Tiedje 1988), we would not expect the tracer addition to elevate DNRA rates significantly.

In contrast to the oxygen and nitrate, ammonium changes in the flow-through cores did not match those along hyporheic flow lines. Ammonium was not measured in 2000, but data from November 1996 to July 1997 (Storey 2001) showed that ammonium was patchy in the hyporheic zone. Surface concentrations varied between 0.08 and 0.13 mg L^{-1} ; in July, the concentration decreased from 0.15 mg L^{-1} in pipe A to 0.06 mg L^{-1} in pipe D, but in other seasons there was no consistent trend. In contrast, water flowing through the sediment cores always increased in ammonium. This difference also may be related to the lability of POM in the cores. More labile POM would favour heterotrophy over nitrification (Schramm et al. 1996), which might both increase ammonification of organic nitrogen and depress the utilisation of this ammonium. Further, more labile POM may favour DNRA over denitrification, since it would provide a greater supply of electrons (Tiedje 1988), and thus would add another source of ammonium in the cores.

Therefore we must conclude that certain processes seen in the flow-through experiments do not accurately represent those occurring in the field. In particular, DNRA is likely to be less important in the field, and nitrification may be more important, probably due to the lower amount of labile POM. In the Speed River, it appears that POM typically is buried gradually (D.D. Williams, unpublished data), therefore we would rarely expect deposits of fresh, labile POM in the hyporheic zone. However, in many other streams (e.g., Naegeli et al. 1995), POM is buried in hyporheic sediments during storms or spates, which raise the total amount of sediment POM by 2–3 times, and likely increase the amount of labile POM by an even greater factor. In such streams it is possible that DNRA occurs for a period after the fresh POM is deposited. In streams that receive input of highly labile DOC from agricultural or domestic effluent, we might also expect DNRA to occur within hyporheic sediments (e.g., Kelso et al. 1999). Therefore, although processes observed in these flow-through experiments probably do not represent typical con-

ditions in the Speed, they are likely within the range of processes that occur after deposition events in many streams.

Microbial responses to the downwelling–upwelling divide

Previous field studies at this Speed River site using salt tracers and natural profiles of conductivity and alkalinity (Storey 2001) have shown that while downwelling and upwelling zones are connected by hyporheic flow lines, the upwelling zone also has a strong influence of true groundwater that produces distinctly different physicochemical conditions. The location of this divide between more surface water-influenced and more groundwater-influenced conditions was shown to shift between seasons. We were interested whether this divide and its seasonal movement would be apparent in the types and rates of microbial processes in hyporheic sediments. In November, field physicochemical data indicated a somewhat diffuse boundary between pipes B and C, suggesting that pipe A and B(20–80) belonged to a surface water-influenced environment whereas pipes C and D belonged to a more strongly groundwater-influenced environment. Microbial processes showed a clearer breakline, also between pipes C and D. Probably because of their higher initial oxygen and nitrate, A(20, 40, 60), B(20) and the surface cores all had significantly different rates of respiration, denitrification rate, and rates of ammonium and ferrous iron production, than pipes C and D. B(40) and B(60) acted like the upwelling zone cores in some ways (ferrous iron and ammonium production, response of denitrification rate to nitrapyrin), but in other ways (e.g., respiration rate, denitrification rate) were indistinguishable from the downwelling zone cores. This behaviour suggests they may be located at the boundary between downwelling and upwelling zones. In all the measured processes they were highly active, which is typical of ecological boundaries and ecotones (Gibert et al. 1990). Therefore the November data showed some correspondence between the downwelling–upwelling divide located in the field and the breakline in microbial processes observed in the lab.

Evidence that breaklines in the microbial processes shifted with season was sparse. An unusually wet summer in 2000 meant that the downwelling–upwelling divide (as defined by oxygen, conductivity, etc. in the field) was shallower in August than in November. Among the flow-through cores in August, A(20) and B(20) were the only two in which denitrification appeared to be oxygen-limited, and these showed very little nitrate loss, compared with almost complete nitrate loss in all the other cores. This suggests that in August, the breakline in microbial processes was between 20 and 40 cm deep at pipes A and B. However we cannot draw definite conclusions based on the evidence of only two cores.

Comparison with other stream systems

Most previous studies have been done at relatively pristine sites, that, relative to the Speed River, have low surface water nitrate-N (e.g. 0.02 mg L^{-1} , Triska et al. 1993;

0.099 mg L⁻¹, Jones et al. 1995; 0.15 mg L⁻¹, Valett et al. 1996; <0.01 mg L⁻¹, Wondzell and Swanson 1996; cf. 0.3 mg L⁻¹ in our study), low POM (0.012–0.155 g C L sediment⁻¹, Jones et al. 1995; 0.14–0.27 g C L sediment⁻¹, Fuss and Smock 1996; cf. 1.0–3.3 g C L sediment⁻¹ in our study) and high subsurface water flow velocities (0.24–0.88 m h⁻¹, Triska et al. 1993; 0.126–4.5 m h⁻¹, Jones et al. 1995; cf. 0.01–0.02 m h⁻¹ in our study). In most of these studies, DO remained relatively high throughout the hyporheic zone (3.9 mg L⁻¹, Jones et al. 1995; 5.5 mg L⁻¹, Wondzell and Swanson 1996), and nitrate increased along subsurface flow lines (from 0.099 to 0.173 mg L⁻¹, Jones et al. 1995; from 0.01 to 0.02 mg L⁻¹ along gravel-bar flow line in summer, Wondzell and Swanson 1996). In the Speed River, however, nitrate, ammonium, DO and DOC all decreased to low levels along an 8–10 m-long hyporheic flow path. This is due to a number of factors. First, because interstitial flow velocities were 10–100 times lower than the other studies described here, hyporheic microbial activity had ample time to remove oxygen from the inflowing water. Second, probably because POM was higher in Speed River sediments than at most other sites, respiration rates were up to twice as high (cf. Naegeli and Uehlinger 1997; Fellows et al. 2001), causing rapid oxygen uptake. Nitrification was likely of minor importance in the Speed (although rates could not be measured accurately in the flow-through experiments), because of competition with heterotrophs for oxygen, and because of relatively low concentrations of ammonium brought in by groundwater and surface water. The relative importance of nitrification as a source of nitrate was further decreased by the moderately high concentration of nitrate in inflowing surface water. Denitrification, in contrast, was of major importance because of this moderately high nitrate concentration. Although denitrification rates were lower than the 4–7 ng N g sediment⁻¹ h⁻¹ reported by Holmes et al. (1996) the long water residence time meant that the cumulative effect was greater; Holmes et al. (1996) estimated that although denitrification removed 5–40% of nitrate produced by nitrification, nitrate still increased along flow lines, whereas we found that nitrate decreased from 0.3 mg L⁻¹ or more in surface water, to less than 0.01 mg L⁻¹ at the end of the hyporheic flow line. That the hyporheic zone at this site is a nitrogen sink, rather than a source, agrees with results from other N-rich streams (Pinay et al. 1994; Hill et al. 1998), and fits the conceptual framework of Jones and Holmes (1996).

Hill et al. (1998) noted a large unused potential for denitrification in the hyporheic zone of a N-rich southern Ontario stream. Laboratory measurements and field observations lead us to the same conclusion regarding the Speed River. The influence of hyporheic processes on whole stream metabolism and nutrient spiralling at this site is clearly limited by the low subsurface flow rates, rather than the rate of hyporheic processes (Findlay 1995). Although hyporheic processing removes almost all oxygen and nitrogen, a maximum of only 0.01–0.2% of stream water discharge is exchanged with the hyporheic zone in this 10 m riffle (Storey et al. 2003), meaning that 5–100 km would be required for 100% exchange. Because of this low hydrologic exchange rate and the high denitrification rates shown in surface sediments, this Speed River site appears to fit the model of Hill et al. (1998). This model, based on high denitrification rates at the stream bed surface,

states that in N-rich streams, surface water storage zones have more influence than hyporheic storage over nitrate retention.

Acknowledgements

We thank the McKenzie family for permission to use their stream and water well, Robert Drimmie and William Mark from University of Waterloo for use of, and assistance with, their Isotope Ratio Mass Spectrometer, Lucie Sliva and Katarina Magnusson for help with field work. We thank two anonymous reviewers for their helpful comments. This research was supported by a National Sciences and Engineering Research Council of Canada grant to D.D. Williams.

References

- Baker M.A., Dahm C.N. and Valett H.M. 2000. Anoxia, anaerobic metabolism, and biogeochemistry of the stream-water-groundwater interface. In: Jones J.B. and Mulholland P.J. (eds) *Streams and Ground Waters*. Academic Press, Boston, pp. 259–283.
- Bishop J.E. and Hynes H.B.N. 1969. Upstream movements of the benthic invertebrates in the Speed River, Ontario. *J. Fish. Res. Board Canada* 26: 279–298.
- Chestnut T.J. and McDowell W.H. 2000. C and N dynamics in the riparian and hyporheic zones of a tropical stream, Luquillo Mountains, Puerto Rico. *J. N. Am. Benthol. Soc.* 19: 199–214.
- Dent C.L., Schade J.D., Grimm N.B. and Fisher S.G. 2000. Subsurface influences on surface biology. In: Jones J.B. and Mulholland P.J. (eds) *Streams and Ground Waters*. Academic Press, Boston, pp. 381–402.
- Duff J.H. and Triska F.J. 1990. Denitrification in sediments from the hyporheic zone adjacent to a small forested stream. *Can. J. Fish. Aquat. Sci.* 47: 1140–1147.
- Duff J.H. and Triska F.J. 2000. Nitrogen biogeochemistry and surface-subsurface exchange in streams. In: Jones J.B. and Mulholland P.J. (eds) *Streams and Ground Waters*. Academic Press, Boston, pp. 197–220.
- Fellows C.S., Valett H.M. and Dahm C.N. 2001. Whole-stream metabolism in two montane streams: contribution of the hyporheic zone. *Limnol. Oceanogr.* 46: 523–531.
- Findlay S. 1995. Importance of surface–subsurface exchange in stream ecosystems: The hyporheic zone. *Limnol. Oceanogr.* 40: 159–164.
- Findlay S. and Sobczak W.V. 2000. Microbial communities in hyporheic sediments. In: Jones J.B. and Mulholland P.J. (eds) *Streams and Ground Waters*. Academic Press, Boston, pp. 284–306.
- Fraser B.F. and Williams D.D. 1998. Seasonal boundary dynamics of a groundwater/surface-water ecotone. *Ecology* 79: 2019–2031.
- Fraser B.F., Williams D.D. and Howard K.W.F. 1996. Monitoring biotic and abiotic processes across the hyporheic/groundwater interface. *Hydrogeol. J.* 4: 36–50.
- Fuss C.L. and Smock L.A. 1996. Spatial and temporal distribution of microbial respiration rates in a blackwater stream. *Freshwat. Biol.* 36: 339–349.
- Gibert J., Dole-Olivier M.-J., Marmonier P. and Vervier P. 1990. Surface water–groundwater ecotones. In: Naiman R.J. and Decamps H. (eds) *The Ecology and Management of Aquatic–Terrestrial Ecotones*. UNESCO and the Parthenon Publishing Group, Park Ridge, New Jersey, pp. 199–225.
- Halda-Alija L., Hendricks S.P. and Johnston T.C. 2001. Spatial and temporal variations of *Enterobacter* genotypes in sediments and the underlying hyporheic zone of an agricultural stream. *Microb. Ecol.* 42: 286–294.
- Hill A.R., Labadia C.F. and Sanmugadas K. 1998. Hyporheic zone hydrology and nitrogen dynamics in relation to the streambed topography of a N-rich stream. *Biogeochemistry* 42: 285–310.

- Hinkle S.R., Duff J.H., Triska F.J., Laenen A., Gates E.B., Bencala K.E., Wentz D.A. and Silva S.R. 2001. Linking hyporheic flow and nitrogen cycling near the Willamette River – a large river in Oregon, USA. *J. Hydrol.* 244: 157–180.
- Holmes R.M., Jones J.B., Fisher S.G. and Grimm N.B. 1996. Denitrification in a nitrogen-limited stream ecosystem. *Biogeochemistry* 33: 125–146.
- Jones J.B. 1995. Factors controlling hyporheic respiration in a desert stream. *Freshwat. Biol.* 34: 91–99.
- Jones J.B. and Holmes R.M. 1996. Surface–subsurface interactions in stream ecosystems. *Trends Ecol. Evol.* 11: 239–242.
- Jones J.B., Fisher S.G. and Grimm N.B. 1995. Nitrification in the hyporheic zone of a desert stream ecosystem. *J. N. Am. Benthol. Soc.* 14: 249–258.
- Kelso B.H.L., Smith R.V. and Laughlin R.J. 1999. Effects of carbon substrates on nitrite accumulation in freshwater sediments. *Appl. Environ. Microbiol.* 65: 61–66.
- Malhi S.S. and Nyborg M. 1983. Release of mineral N from soils: influence of inhibitors of nitrification. *Soil Biol. Biochem.* 15: 581–585.
- McMahon P.B., Tindall J.A., Collins J.A. and Lull K.J. 1995. Hydrologic and geochemical effects on oxygen uptake in bottom sediments of an effluent-dominated river. *Water Resour. Res.* 31: 2561–2569.
- Morrice J.A., Valett H.M., Dahm C.N. and Campana M.E. 1997. Alluvial characteristics, groundwater–surface water exchange and hydrological retention in headwater streams. *Hydrol. Proc.* 11: 253–267.
- Naegeli M.W. and Uehlinger U. 1997. Contribution of the hyporheic zone to ecosystem metabolism in a prealpine gravel-bed river. *J. N. Am. Benthol. Soc.* 16: 794–804.
- Naegeli M.W., Hartmann U., Meyer E.I. and Uehlinger U. 1995. POM-dynamics and community respiration in the sediments of a floodprone prealpine river (Necker, Switzerland). *Arch. Hydrobiol.* 133: 339–347.
- Nakajima T. 1979. Denitrification by the sessile microbial community of a polluted river. *Hydrobiologia* 66: 57–64.
- Nelson D.W. and Sommers L.E. 1996. Total carbon, organic carbon and organic matter. In: *Methods of Soil Analysis. Part 3: Chemical Methods*. Soil Sci. Soc. Am. and Am. Soc. Agronomy, Madison, WI, pp. 961–1010.
- Nielsen L.P. 1992. Denitrification in sediment determined from nitrogen isotope pairing. *FEMS Microbiol. Ecol.* 86: 357–362.
- Pinay G., Haycock N.E., Ruffinoni C. and Holmes R.M. 1994. The role of denitrification in nitrogen removal in river corridors. In: Mitsch W.J. (ed) *Global Wetlands: Old World and New*. Elsevier, Amsterdam, pp. 1–7116.
- Pusch M.H.E. 1987. Die Besiedlung des hyporheischen Interstitals in einem Schwarzwaldbach. Diploma thesis, University of Freiberg.
- Pusch M. 1996. The metabolism of organic matter in the hyporheic zone of a mountain stream, and its spatial distribution. *Hydrobiologia* 323: 107–118.
- Riemer M. and Harremoës P. 1978. Multi-component diffusion in denitrifying biofilms. *Progr. Water Tech.* 10: 149–165.
- Sabater S., Guasch H., Romání A. and Muñoz I. 2002. The effect of biological factors on the efficiency of river biofilms in improving water quality. *Hydrobiologia* 469: 149–156.
- Schramm A., Larsen L.H., Revsbech N.P., Ramsing N.B., Amann R. and Schleifer K.H. 1996. Structure and function of a nitrifying biofilm as determined by *in situ* hybridisation and the use of micro-electrodes. *Appl. Environ. Microbiol.* 62: 4641–4647.
- Stanley E.H. and Jones J.B. 2000. Surface–subsurface interactions: past, present, future. In: Jones J.B. and Mulholland P.J. (eds) *Streams and Ground Waters*. Academic Press, Boston, pp. 405–417.
- Stocker Z.S.J. and Williams D.D. 1972. A freezing core method for describing the vertical distribution of sediments in a streambed. *Limnol. Oceanogr.* 17: 136–138.
- Storey R.G. 2001. Spatial and temporal variability in a hyporheic zone: a hierarchy of controls from water flows to meiofauna. PhD Thesis, University of Toronto, 230 pp.
- Storey R.G., Howard K.W.F. and Williams D.D. 2003. Factors controlling riffle-scale hyporheic exchange flows and their seasonal changes in a gaining stream: a three-dimensional groundwater flow model. *Water Resour. Res.* 39 (2): Art. No. 1034.

- Tiedje J.M. 1988. Ecology of denitrification and dissimilatory nitrate reduction to ammonium. In: Zehnder A.J.B. (ed) *Biology of Anaerobic Microorganisms*. John Wiley & Sons, Toronto, pp. 179–244.
- Triska F.J., Duff J.H. and Avanzino R.J. 1990. Influence of exchange flow between the channel and hyporheic zone on NO_3^- production in a small mountain stream. *Can. J. Fish. Aquat. Sci.* 11: 2099–2111.
- Triska F.J., Duff J.H. and Avanzino R.J. 1993. The role of water exchange between a stream channel and its hyporheic zone in nitrogen cycling at the terrestrial–aquatic interface. *Hydrobiologia* 251: 167–184.
- Valett H.M., Morrice J.A., Dahm C.N. and Campana M.E. 1996. Parent lithology, surface–groundwater exchange, and nitrate retention in headwater streams. *Limnol. Oceanogr.* 41: 333–345.
- Vannelli T. and Hooper A.B. 1992. Oxidation of nitrapyrin to 6-chloropicolinic acid by the ammonia-oxidising bacterium *Nitrosomonas europaea*. *Appl. Environ. Microbiol.* 58: 2321–2326.
- Vannelli T. and Hooper A.B. 1993. Reductive dehalogenation of the trichloromethyl group of nitrapyrin by the ammonia-oxidizing bacterium *Nitrosomonas europaea*. *Appl. Environ. Microbiol.* 59: 3597–3601.
- Ventullo R.M. and Rowe J.J. 1982. Denitrification potential of epilithic communities in a lotic environment. *Current Microbiol.* 7: 29–33.
- Wondzell S.M. and Swanson F.J. 1996. Seasonal and storm dynamics of the hyporheic zone of a 4th-order mountain stream. II: nitrogen cycling. *J. N. Am. Benthol. Soc.* 15: 20–34.